XI International Conference on Computational Plasticity. Fundamentals and Applications
COMPLAS XI
E. Oñate, D.R.J. Owen, D. Peric and B. Suárez (Eds)

DYNAMIC RECRYSTALLIZATION MODEL DURING HOT WORKING BY COUPLING PHASE-FIELD METHOD AND FINITE ELEMENT METHOD

TOMOHIRO TAKAKI*

*Mechanical and System Engineering, Graduate School of Science and Technology
Kyoto Institute of Technology
Matsugasaki, Sakyo, Kyoto 606-8585, Japan
e-mail: takaki@kit.ac.jp, http://www.cis.kit.ac.jp/˜takaki/

Key words: Dynamic Recrystallization, Hot Working, Microstructure, Multi-Phase-Field Method, Finite Element Method, Multiscale Modeling

Abstract. Multiscale model for hot–working, which can investigate the macroscopic mechanical behavior based on the microstructure evolution, has been developed by coupling the finite element (FE) method and phase–field (PF) method. Here, the microstructure evolutions in dynamic recrystallization are simulated by the multi–phase–field-dynamic recrystallization (MPF–DRX) model. The microscopic simulations are performed in every element used in the finite element simulations to calculate the macroscopic mechanical behaviors.

1 INTRODUCTION

During hot–working of low–to–medium stacking fault energy metal, the dynamic recrystallization (DRX) occurs, where the plastic deformation due to dislocation accumulation and the nucleation and growth of recrystallized grain occur simultaneously [1]. The macroscopic mechanical behavior during DRX shows a characteristic stress – strain curve, or single and/or multiple peak curves are generated depending on the initial grain size, the strain rate and the temperature [2]. Because these macroscopic stress – strain curves are largely affected by the microstructure evolution, it is key for the working process design to develop a multiscale numerical model for the hot–working. There are roughly two kinds of multiscale method: one is by finite element method [3, 4, 5, 6, 7], which mainly focuses on the macroscopic mechanical behavior, and the other is by grain growth model [9, 10, 11, 12, 13, 14, 15, 16, 17], which focuses on the microstructure evolution.

In finite element simulations considering the DRX microstructure evolution during hot–working [3, 4, 5, 6, 7], the information of microstructure, such as average grain size, recrystallization volume fraction, stored energy (or dislocation density) and so on, is incorporated into the model through the constitutive equation and the DRX microstructural

information is updated as a function of strain, strain rate and temperature. To increase the accuracy of these models in more practical hot–working, it is key to properly incorporate the information of DRX microstructure evolutions, which largely depends on the stress and thermal history, into the constitutive equation.

In DRX simulations using grain growth model [9, 10, 11, 12, 13, 14, 15, 16, 17], the nucleation and growth of DRX grains, or realistic DRX microstructure evolution, are simulated and the macroscopic stress–strain curve is calculated from the average dislocation density in the computational domain. As a grain growth model, Cellular Automata (CA) is widely employed [9, 10, 11, 12, 13, 14, 15]. We have developed the MPF–DRX model [16, 17] using multi–phase–field (MPF) method instead of CA and confirmed that the MPF-DRX model can be applied to the transient deformation where strain and temperature change rapidly during deformation [18].

In this study, we develop multiscale DRX model coupling above two types of DRX models, where the DRX microstructure evolution is simulated by MPF–DRX model and the macroscopic mechanical behavior is calculated by large deformation finite element analysis, where the conventional J_2–flow theory is used as the constitutive equation.

2 COUPLING OF MPF–DRX MODEL AND FE METHOD

Figure 1 shows an image of the multiscale simulation using MPF–DRX model and FE method.

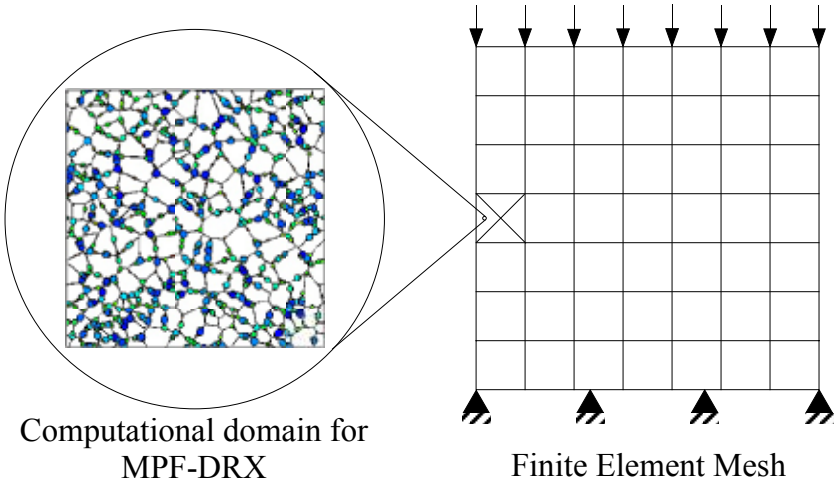

Figure 1: Image of multiscale simulation

The MPF–DRX simulations are performed in all finite elements used in FE simulation. Because the crossed-triangle element is employed in the present FE simulation, in the example of Fig.1, the computational domains with 196 numbers ($= 7 \times 7 \times 4$) are prepared and the MPF–DRX simulations are performed in all 196 domains. The equivalent strain rate $\dot{\bar{\varepsilon}}$ and temperature T, which are different in every element, are transferred from

FE simulation to MPF–DRX simulation and the tangent modulus $d\bar{\sigma}/d\bar{\varepsilon}$ which is the slope of the uniaxial stress–strain curve is transferred from MPF–DRX simulation to FE simulation.

3 MPF–DRX MODEL

In the MPF–DRX model [16], the grain growth driven by stored energy is simulated by the MPF method [21] and the local dislocation density evolution due to plastic deformation and dynamic recovery (DRV) is expressed by the Kocks–Mecking (KM) model [19]. A macroscopic stress-strain curve is obtained from the Bailey–Hirsch equation [20] using average dislocation density in all computational domain.

3.1 MPF model

A polycrystalline system including N grains is indicated by N phase–field variables. The ith grain is indicated by the phase field ϕ_i, where ϕ_i takes values of 1 inside the ith grain, 0 inside the other grains, and $0 < \phi_i < 1$ at the grain boundary. The evolution equation of ϕ_i is expressed by [21]

$$\dot{\phi}_i = -\sum_{j=1}^{n} \frac{2M_{ij}^{\phi}}{n} \left[\sum_{k=1}^{n} \left\{ \left(W_{ik} - W_{jk}\right) \phi_k + \frac{1}{2} \left(a_{ik}^2 - a_{jk}^2\right) \nabla^2 \phi_k \right\} - \frac{8}{\pi} \sqrt{\phi_i \phi_j} \Delta f_{ij} \right]. \quad (1)$$

where n is the number of phase–field variables larger than 0 at the lattice point, a_{ij}, W_{ij}, and M_{ij}^{ϕ} are the gradient coefficients, the height of double–well potentials and the phase–field mobilities related to the grain boundary thickness δ, grain boundary energy γ and grain boundary mobility M, respectively, by

$$a_{ij} = \frac{2}{\pi} \sqrt{2\delta\gamma}, \quad W_{ij} = \frac{4\gamma}{\delta}, \quad M_{ij}^{\phi} = \frac{\pi^2}{8\delta} M. \quad (2)$$

Here, δ, γ and M are assumed to be constant at all boundaries and Eq.(2) is true only for $i \neq j$ and the diagonal components are zero. The driving force Δf_{ij} can be obtained as $\Delta f_{ij} = 1/2\mu b^2(\rho_i - \rho_j)$, where μ is the shear modulus, b is the magnitude of the Burgers vector, and ρ_i and ρ_j are the dislocation densities in ith and jth adjacent grains, respectively.

3.2 Dislocation evolution and macroscopic stress

The accumulation of dislocations due to plastic deformation and DRV is expressed by the KM model [19] as the relationship between the local dislocation density ρ_i in the ith grain and the true strain ε;

$$\frac{d\rho_i}{d\varepsilon} = k_1 \sqrt{\rho_i} - k_2 \rho_i. \quad (3)$$

Here, the first term on the right–hand side expresses the work hardening, where k_1 is a constant that represents hardening. The second term is the DRV term, where k_2 is a

function of the temperature T and the strain rate $\dot{\varepsilon}$. [9] . Macroscopic stress is related to the average dislocation density $\bar{\rho}$ as

$$\sigma = \alpha\mu b\sqrt{\bar{\rho}}, \tag{4}$$

where α is the dislocation interaction coefficient of approximately 0.5. From eqs. (3) and (4), a macroscopic stress–strain curve can be determined.

3.3 Nucleation of DRX grains

It is assumed that the nucleation of recrystallized grains occurs only with the bulging of a grain boundary in the present model. Therefore, when the dislocation density at a grain boundary exceeds its critical value ρ_c, or

$$\rho_c = \left(\frac{20\gamma\dot{\varepsilon}}{3blM\tau^2}\right)^{1/3}, \tag{5}$$

nuclei are in placed at a grain boundary by following the nucleation rate per unit area of a grain boundary [9]

$$\dot{n} = c\dot{\varepsilon}^d \exp(-\frac{\omega}{T}), \tag{6}$$

where $\tau = 0.5\mu b^2$ is the line energy of a dislocation, l is the mean free path of mobile dislocation expressed by $l = 10/(0.5\sqrt{\rho_0})$, [9] and c, d and ω are constants.

4 FINITE ELEMENT METHOD

To evaluate the macroscopic mechanical behavior during hot–working process, the elasto–plastic large deformation simulation is performed by finite element method. Here, the conventional J_2–flow theory is employed as the constitutive equation, where the elastic strain rate $\dot{\varepsilon}^e_{ij}$ and plastic strain rate $\dot{\varepsilon}^p_{ij}$ are derived from the generalized Hook's low and the flow low and the Mises yield function, respectively. The relation between the Jaumann rate of Kirchoff stress S_{ij} and strain rate $\dot{\varepsilon}_{ij}$ is indicated as follow:

$$S_{ij} = \left(D^e_{ijkl} - \frac{2G}{g}\sigma'_{ij}\sigma'_{kl}\right)\dot{\varepsilon}_{kl}, \tag{7}$$

where D^e_{ijkl}, σ'_{ij} and G are the elastic coefficient tensor, the deviatoric Cauchy stress tensor and shear modulus expressed as $G = E/\{2(1+\nu)\}$, respectively. In addition, g is expressed by

$$g = \frac{2}{3}\bar{\sigma}^2\left(1 + \frac{h}{2G}\right), \quad \bar{\sigma}^2 = \frac{3}{2}\sigma'_{ij}\sigma'_{ij}, \tag{8}$$

where, taking into account the uniaxial test and non–compressibility,

$$\frac{1}{h} = \frac{3}{2}\left(\frac{1}{E_t} - \frac{1}{E}\right), \tag{9}$$

can be obtaind. Here, E_t is the tangential coefficient in the true stress and true strain curve, or $E_t = d\sigma/d\varepsilon$, and is calculated in the MPF–DRX simulation. Therefore, in the present FE simulation, we don't need the uniaxial constitutive equation obtained by uniaxial test, which is required in the normal FE simulation.

Because the strain rate dependency is contained in the MPF–DRX simulation, the strain rate independent constitutive equation is used in the FE simulation. In this study, furthermore, an isothermal condition is assumed and, therefore, the thermal conduction equation is not shown here.

5 NUMERICAL SIMULATIONS

To confirm the accuracy of the present model, the uniaxial compression simulations in a plane stress condition of copper [18] are performed for a single crossed–triangle element. The constant strain rates $\dot{\varepsilon}$ are set to be 0.001, 0.003, 0.01, 0.03 and 0.1/s in the isothermal condition $T = 800$ K. The time step is determined as $\Delta t = \Delta x^2/\left(4a^2M^{\phi}\right)$ from Eq.(1). Because the strain increment $\Delta\varepsilon$ is calculated as $\Delta\varepsilon = \dot{\varepsilon}\Delta t$, $\Delta\varepsilon$ changes depend on the $\dot{\varepsilon}$. Young's modulus E is derived as $E = 0.5\alpha\mu bk_1$ from Eqs.(3), which is a gradient of true stress and true strain curve at $\varepsilon = 0$, and (4) and Poisson's ration is set to be 0.3.

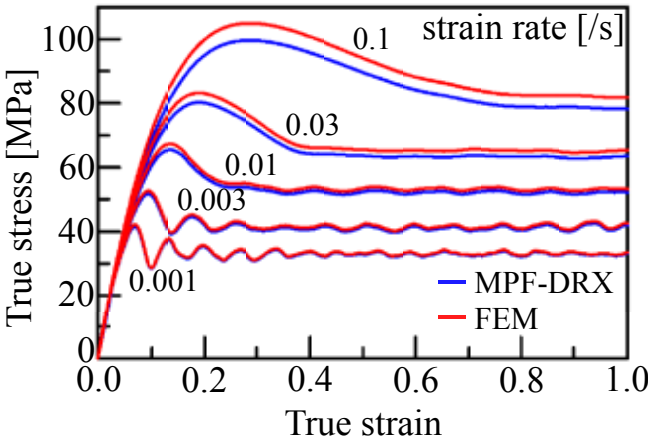

Figure 2: Stress–strain curves calculated by MPF–DRX model and FE method

Figure 2 shows the true stress and true strain relations for five different strain rates. Although the present simulation is compression, stress and strain are indicated as positive value. From Fig.2, the characteristic stress–strain curves in DRX, where the transition from the multiple peaks to the single peak occurs with increasing the strain rate, can be observed. Red lines are the results of MPF–DRX simulation and blue lines are the results of FE simulation used the results of MPF–DRX simulation. The good agreements between red and blue lines are confirmed especially in slow strain rate region.

Figure 3 shows the DRX microstructure evolution for $\dot{\varepsilon} = 0.01$/s. The color indicates the DRX cycle defined in Ref. [17].

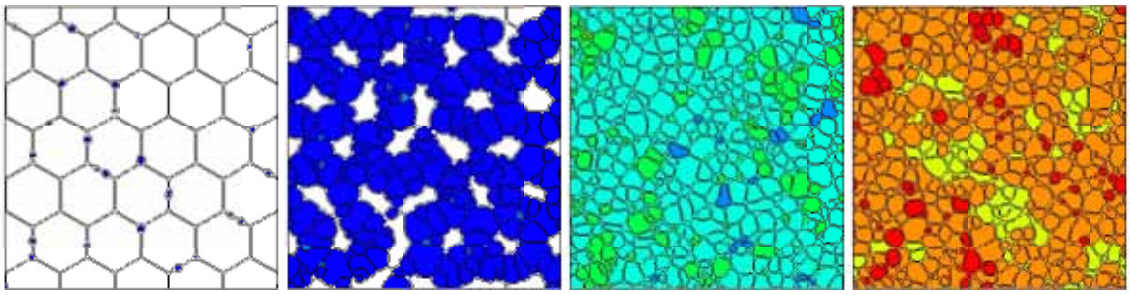

(a) ε = -0.1 (b) ε = -0.2 (c) ε = -0.5 (d) ε = -1.0

Figure 3: DRX microstructure evolutions ($\dot{\varepsilon} = 0.01$)

From Figs.2 and 3, it is confirmed that the present model can simulate the microstructure evolution and the macroscopic mechanical behavior simultaneously. However, the results shown in Figs.2 and 3 can be calculated only by the MPF–DRX model. The novel point of the present coupling model is that the model can simulate the different microstructure evolution for every finite element in the nonuniform deformation simulation.

6 CONCLUSIONS

The novel multiscale model, which can evaluate the macroscopic mechanical behavior based on the microstructure evolution considering the DRX in hot–working process, has been developed. Here, the MPF–DRX model has been incorporated into the large deformation FE method with the conventional J_2 flow theory as the constitutive equation. The uniaxial compression simulations using one crossed–triangle element were performed to confirm the accuracy of the developed model.

As future work, the model will be extended to the nonuniform and nonisothermal deformation condition.

REFERENCES

[1] F. J. Humphreys and M. Hatherly: Recrystallization and Related Annealing Phenomena, Elsevier, (2004), 415.

[2] T. Sakai and J. J. Jonas, Dynamic recrystallization: mechanical and microstructural considerations, *J. Mater. Process. Technol.*, (1984) **32**:189–209.

[3] K. Karhausen and R. Kopp, Model for integrated process and microstructure simulation in hot forming, *Steel Res.*, (1992) **63**:247–256.

[4] M. Glowacki, R. Kuziak, Z. Malinowski and M. Pietrzyk, Modelling of heat transfer, plastic flow and microstructural evolution during shape rolling, *Acta Metall.*, (1995) **53**:159–166.

[5] F. P. E. Dunne, M. M. Nanneh and M. Zhou, Anisothermal large deformation constitutive equations and their application to modelling titanium alloys in forging, *Philos. Mag. A*, (1997) **75**:587–610.

[6] E. P. Busso, A continuum theory for dynamic recrystallization with microstructure-related length scales, *Int. J. Plast.*, (1998) **14**:319–353.

[7] C. M. Sellars and Q. Zhu, Microstructural modelling of aluminium alloys during thermomechanical processing, *Mater. Sci. Eng., A*, (2000) **280**:1–7.

[8] J. R. Cho, H. S. Jeong, D. J. Cha, W. B. Bae and J. W. Lee, Prediction of microstructural evolution and recrystallization behaviors of a hot working die steel by FEM, *J. Mater. Process. Technol.*, (2005) **160**:1–8.

[9] R. Ding and Z. X. Guo, Coupled quantitative simulation of microstructural evolution and plastic flow during dynamic recrystallization, *Acta Mater.*, (2001) **49**:3163–3175.

[10] R. Ding and Z. X. Guo, Microstructural evolution of a Ti–6Al–4V alloy during thermomechanical processing, *Mater. Sci. Eng. A*, (2004) **365**:172–179.

[11] M. Qian and Z. X. Guo, Cellular automata simulation of microstructural evolution during dynamic recrystallization of an HY-100 steel, *Mater. Sci. Eng. A*, (2004) **365**:180–185.

[12] G. Kugler and R. Turk, Modeling the dynamic recrystallization under multi-stage hot deformation, *Acta Mater.*, (2004) **52**:4659–4668.

[13] R. L. Goetz, Particle stimulated nucleation during dynamic recrystallization using a cellular automata model, *Scr. Mater.*, (2005) **52**:851–856.

[14] N. Xiao, C. Zheng, D. Li and Y. Li, A simulation of dynamic recrystallization by coupling a cellular automaton method with a topology deformation technique, *Comp. Mater. Sci.*, (2008) **41**:366–374.

[15] C. Zheng, N. Xiao, D. Li and Y. Li, Microstructure prediction of the austenite recrystallization during multi-pass steel strip hot rolling: A cellular automaton modeling, *Comp. Mater. Sci.*, (2008) **44**:507–514.

[16] T. Takaki, T. Hirouchi, Y. Hisakuni, A. Yamanaka and Y. Tomita, Multi-Phase-Field Model to Simulate Microstructure Evolutions during Dynamic Recrystallization, *Mater. Trans.*, (2008) **49**:2559–2565.

[17] T. Takaki, T. Hirouchi, Y. Hisakuni, A. Yamanaka and Y. Tomita, Multi-phase–field simulations for dynamic recrystallization, *Comput. Mater. Sci.*, (2009) **45**:881–888.

[18] T. Takaki, A. Yamanaka and Y. Tomita, Multi-Phase-Field Simulations of Dynamic Recrystallization during Transient Deformation, *ISIJ Int.*, (2011), *submitted*.

[19] H. Mecking and U. F. Kocks, Kinetics of flow and strain-hardeningstar, *Acta Metall.*, (1981) **29**:1865–1875.

[20] J. E. Bailey and P. B. Hirsch, The dislocation distribution, flow stress, and stored energy in cold-worked polycrystalline silver, *Philos. Mag.*, (1960) **5**:485–497.

[21] I. Steinbach and F. Pezzolla, A generalized field method for multiphase transformations using interface fields, *Physica D*, (1999) **134**:385–393.

[22] Q. Yu and S. K. Esche, A multi-scale approach for microstructure prediction in thermo-mechanical processing of metals , *J. Mater. Process. Technol.*, (2005) **169**:493–502.

[23] H. W. Lee and Y.-T. Im, Numerical modeling of dynamic recrystallization during nonisothermal hot compression by cellular automata and finite element analysis, *Int. J. Mech. Sci.*, (2010) **52**:1277–1289.